PHYSICAL REVIEW D

PARTICLES AND FIELDS

THIRD SERIES, VOLUME 26, NUMBER 3 1 AUGUST 1982

Study of the reaction $\nu_\mu d \to \mu^- pp_s$

K. L. Miller,* S. J. Barish,† A. Engler, R. W. Kraemer, and B. J. Stacey‡
Carnegie-Mellon University, Pittsburgh, Pennsylvania 15213

M. Derrick, E. Fernandez, L. Hyman, G. Levman,§ D. Koetke,‖
B. Musgrave, P. Schreiner,¶ R. Singer,¶ A. Snyder,** and S. Toaff††
Argonne National Laboratory, Argonne, Illinois 60439

D. D. Carmony, G. M. Radecky,‡‡ V. E. Barnes, and A. F. Garfinkel
Purdue University, W. Lafayette, Indiana 47907

R. Ammar, D. Coppage, D. Day, R. Davis, N. Kwak, and R. Stump
University of Kansas, Lawrence, Kansas 66045

(Received 25 January 1982)

This paper reports a determination of the axial-vector form factor of the nucleon using the momentum-transfer distribution for 1737 events of the type $\nu_\mu d \to \mu^- pp_s$. The events were obtained from a 2.4×10^6-frame exposure of the Argonne 12-foot bubble chamber to a neutrino beam at the Argonne Zero Gradient Synchrotron. After fitting and applying selection criteria, the background was estimated to be at the 2% level. The axial-vector mass in the dipole parametrization was measured to be $M_A = 1.00\pm0.05$ GeV/c^2, in good agreement both with earlier measurements from this experiment and with other recent results. A test of the conserved-vector-current hypothesis, made by simultaneously fitting M_A and M_V using dipole form factors, gave $M_A = 0.80\pm0.10$ GeV/c^2 and $M_V = 0.96 \pm 0.04$ GeV/c^2.

I. INTRODUCTION

The structure of the nucleon, as measured both by electromagnetic and weak probes, has been a subject of experimental study for many years. The vector form factor, as measured in elastic electron scattering, can be described by a dipole form factor $(1+Q^2/M_V^2)^{-2}$, where Q^2 is the lepton momentum transfer squared, with a characteristic mass of $M_V = 0.84$ GeV/c^2. Although the primary Q^2 dependence is described by this parametrization, the data deviate by a few percent from the pure dipole shape.

Experiments studying quasielastic neutrino scattering, $\nu_\mu n \to \mu^- p$, can measure both the vector and the axial-vector form factors since the weak hadronic charged current contains both of these components. The hypothesis of the isotriplet current relates the vector part of the weak hadronic current to the electromagnetic current, and so, in the simplest analysis, the neutrino experiments just measure the axial-vector form factor.

Quasielastic scattering has been studied in several experiments using complex nuclear targets[1]; we earlier reported an M_A value of 0.95 ± 0.09 GeV/c^2 determined from an experiment using a liquid-deuterium-filled bubble chamber.[2] A second and more recent experiment[3] in deuterium gives $M_A = 1.07\pm0.06$ GeV/c^2. Our analysis of single-pion production[4] in the reaction $\nu_\mu \to \mu^- p\pi^+$ also yields an M_A value close to 1 GeV/c^2.

In this paper we give the final results of our study of quasielastic scattering. The data sample comes from about 2.4×10^6 pictures taken with the 12-foot bubble chamber exposed to a wide-band neutrino beam at the Zero Gradient Synchrotron. The sample of 1737 events, which is about three times larger than we previously published, is the

total data sample from all exposures of the chamber.

II. EXPERIMENTAL ARRANGEMENT

The 12.4-GeV/c^2 proton beam was extracted from the Zero Gradient Synchrotron and focused onto a beryllium target. The positive hadrons produced in the p-Be collisions were focused toward the bubble chamber by two magnetic horns. Neutrinos from the decay of the pions and kaons in the 30-m-long drift space traversed the bubble chamber. A shield in front of the bubble chamber removed all particles except neutrinos.

The neutrino flux was calculated utilizing the measured yields of pions in p-Be collisions and propagating the particles through the horn system and decay tunnel. We estimate the flux uncertainty to be $\pm 15\%$ except at the highest energies where the lack of measurements of K^+ production leads us to assign a $\pm 25\%$ uncertainty. The flux peaks at ~ 0.5 GeV/c^2 and has fallen by an order of magnitude at a neutrino energy of 2 GeV/c^2. A detailed description of the experiment, including the flux measurement, is given in our previous publication.[2]

The film was scanned at each of the collaborating institutions and all one-, two-, and three-prong events recorded. All of the film used for the analysis of quasielastic scattering was double-scanned and some was triple-scanned. The overall scanning efficiency was $(98\pm 2)\%$ for events within a fiducial volume. The scanning efficiency varied slightly with Q^2 is shown in Fig. 1, and an efficiency correction was made as a function of this variable.

For part of the second run, thin tantalum plates were used in the downstream end of the chamber. We discarded all events originating within or downstream of the plates since the boiling around the plate supports degraded the visibility in this region.

To estimate the level of contamination in the quasielastic channel, we studied the quantities $M^2=(E_\mu+E_P+E_{p_s}-M_d)^2-(\vec{P}_\mu+\vec{P}_p+\vec{P}_{p_s})^2$ and α, the angle between the known neutrino beam direction and the reconstructed visible momentum. For neutrino events, both quantities should cluster near zero. Scatter plots of the events in the M^2:α space show such a clustering[2] and give an estimated total background of $(2\pm 2)\%$.

The contamination from events of the channel $\nu_\mu d\to\mu^-\pi^0 pp_s$ was estimated by taking events of the reaction, $\nu_\mu d\to\mu^-\pi^+ pn_s$, deleting the π^+ track, and refitting to the $\nu_\mu d\to\mu^- pp_s$ hypothesis. Monte Carlo simulations were also made. Both methods yielded $(1\pm 1)\%$ for the π^0 background.

All events of the two- and three-prong topologies were fitted to the $\nu_\mu d\to\mu^- pp_s$ hypothesis. Events satisfying this hypothesis were examined by a physicist to verify consistency with such visual information as ionization, decays, or scatters.

For two-prong events, the spectator momentum is not measured, so in the fitting process we assigned 0 ± 50 MeV/c to each Cartesian projection of the spectator momentum. Figure 2 shows the resulting distribution in spectator proton momen-

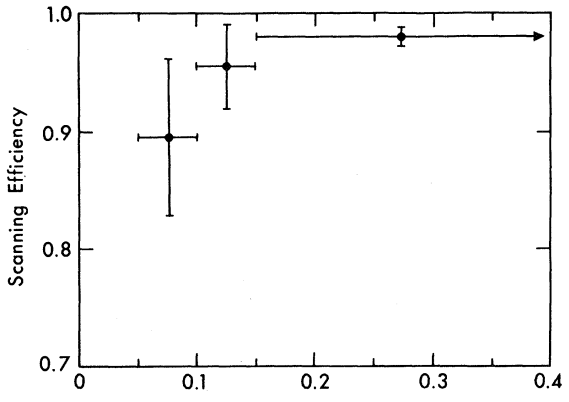

FIG. 1. Scanning efficiency as a function of momentum transfer squared.

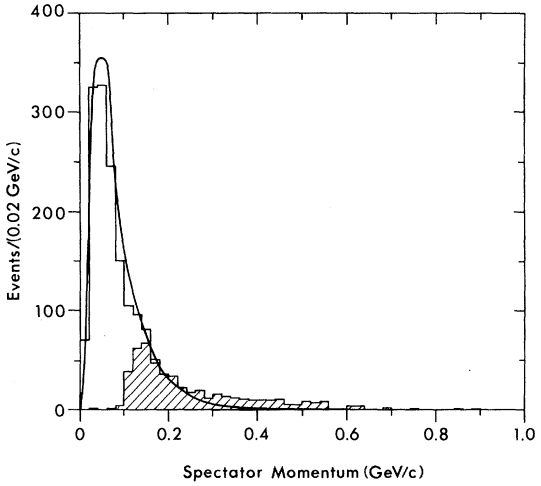

FIG. 2. Spectator-proton momentum distribution. Three-prong events are shown as cross-hatched. The solid curve is the normalized Hulthén distribution.

tum. The three-prong events are shown as cross-hatched. This distribution is well represented by a Hulthén curve except at high spectator momentum. The excess in that region is usually attributed to final-state scattering of the spectator nucleon. Such final-state interactions have no effect on the Q^2 distribution, and therefore no cut on the spectator momentum was made.

After these selections, 1737 events were available for analysis, corresponding to 1792 ± 48 events after corrections for scanning and reconstruction inefficiencies.

III. MEASUREMENT OF THE FORM FACTORS

The matrix element for the hadronic weak current depends on six complex form factors. These are the vector form factor F_V^1, the weak-magnetism form factor F_V^2, the induced scalar form factor F_V^3, the axial-vector form factor F_A^1, the induced pseudoscalar form factor F_P, and the tensor form factor F_A^3. In terms of these form factors, the weak hadronic current can be written as

$$J_\lambda^{\text{hadronic}} \propto \gamma_\lambda F_V^1 + \frac{i\sigma_{\lambda\epsilon}q^\epsilon F_V^2(\mu_p-\mu_n)}{2M} + \frac{q_\lambda F_V^3}{M} + \gamma_\lambda\gamma_5 F_A^1 + \frac{q_\lambda\gamma_5 F_P}{M} + \gamma_5\frac{(P_n+P_p)\lambda}{M}F_A^3 ,$$

where $q\ (=-Q)$ is the four-momentum transfer, M is the nucleon mass, and μ_p and μ_n are the anomalous magnetic moments of the proton and neutron, respectively.

In order to reduce the problem to a manageable level, certain assumptions must be made. These are as follows.

(i) Time-reversal invariance. This implies that all the form factors are real.

(ii) Charge symmetry. As a result, F_V^3 and F_A^3 are imaginary. In combination with (i), charge symmetry then requires that $F_V^3=F_A^3=0$. This is equivalent to saying that second-class currents do not exist.

(iii) Isotriplet-current hypothesis. This assumption relates F_V^1 and F_V^2 to the isovector electromagnetic form factors determined from electron scattering experiments. We use the dipole form and write F_V^1 and $F_V^2=\epsilon(Q^2)/(1+Q^2/M_V{}^2)^2$, where $M_V=0.84$ GeV. $\epsilon(Q^2)$ is a factor that varies between 0.95 and 1.05 and is used to correct for the deviations of the electron scattering data from a pure dipole.

(iv) Small induced pseudoscalar term. We assume, following the suggestion of partial conservation of axial-vector current (PCAC), that F_P is dominated by the pion pole. Since the F_P term is multiplied by the muon mass, the contribution to the cross section is small.

(v) Dipole axial-vector form factor. We take as the parametrization of the axial-vector form factor,

$$F_A^1(Q^2)=\frac{-1.23}{(1+Q^2/M_A{}^2)^2} ,$$

where M_A is a parameter called the axial-vector mass. With the above assumptions, it is the only free parameter.

The cross section for the reaction $\nu_\mu n \to \mu^- p$ can be written as

$$\frac{d\sigma^\nu}{dQ^2}=\frac{M^2G^2\cos^2\theta_C}{8\pi E_\nu{}^2}[A(Q^2)-B(Q^2)(s-u)+C(Q^2)(s-u)^2] ,$$

where G is the weak-interaction coupling constant ($GM^2=1.023\times10^{-5}$), θ_C is the Cabibbo angle ($\cos^2\theta_C=0.94$), A, B, and C are functions of Q^2 and of the form factors F_V^1, F_V^2, and F_A^1, and $(s-u)=4ME_\nu-Q^2-M_\mu{}^2$.

This expression holds for the case of a free neutron and so must be modified in our experiment for the effects of Fermi motion and the Pauli exclusion principle. These corrections will obviously depend weakly on E_ν but strongly on Q^2. Figure 3

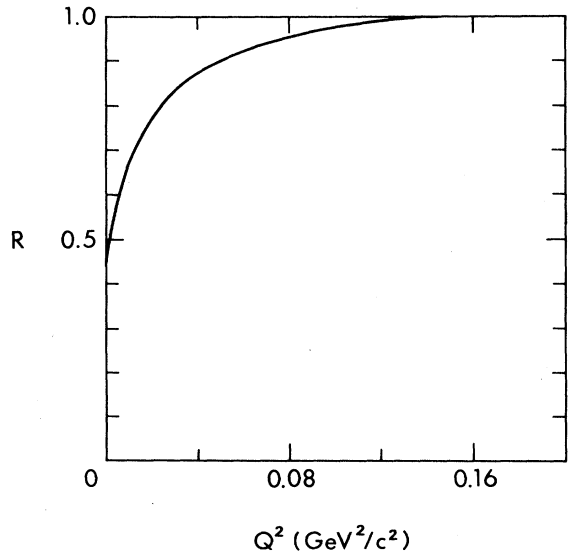

FIG. 3. Deuterium correction factor $R(Q^2)$.

shows the factor $R(Q^2)$ by which we multiply the free-neutron cross section in order to correct for the two deuteron effects mentioned above.

In Fig. 4 we show the weighted number of events as a function of Q^2. The solid curve is obtained from a maximum-likelihood fit of the data to the dipole model. The following likelihood functions (given in logarithmic form) were tried:

$$\mathscr{L}_{\text{rate}} = -\ln(2^{1/2} N_{\text{data}}{}^{1/2}\sigma_N) - \tfrac{1}{2}\left[\frac{N_{\text{data}} - N_{\text{theory}}}{\sigma_n}\right]^2,$$

$$\mathscr{L}_{\text{shape}} = \sum_{i=1}^{N_{\text{data}}} W(Q_i^2)\ln\left[\frac{\frac{d\sigma}{dQ^2}(Q_i^2,E_{\nu i};M_A,M_V)R(Q_i^2)\Phi(E_{\nu i})}{\int\int \frac{d\sigma}{dQ^2}(Q^2,E_\nu;M_A,M_V)R(Q^2)\Phi(E_{\nu i})dQ^2dE_\nu}\right],$$

$$\mathscr{L}_{\text{total}} = \mathscr{L}_{\text{rate}} + \mathscr{L}_{\text{shape}},$$

$$\mathscr{L}_{\text{FI}} = \sum_{i=1}^{N_{\text{data}}} W(Q_i^2)\ln\left[\frac{\frac{d\sigma}{dQ^2}(Q_i^2,E_{\nu i};M_A,M_V)R(Q_i^2)}{\int \frac{d\sigma}{dQ^2}(Q^2,E_\nu;M_A,M_V)R(Q^2)dQ^2}\right],$$

where FI denotes "flux independence." In these equations, σ_N is the experimental error on the expected number of events, $W(Q_i^2)$ is the weight due to scan efficiency, $R(Q_i^2)$ is the deuterium correction, $\Phi(E_{\nu i})$ is the neutrino flux, and $(d\sigma/dQ^2)(Q_i^2,E_{\nu i};M_A,M_V)R(Q_i^2)$ is the differential cross section. One should carefully note the following dependencies. The function $\mathscr{L}_{\text{rate}}$ depends only on the number of events found and not on their distribution in the kinematic space (E_ν,Q^2). The excitation function for the present experiment is in agreement with our earlier result.[2] On the other hand, the function $\mathscr{L}_{\text{shape}}$ does depend on the distribution of the events in the kinematic space (E_ν,Q^2) but not on the overall normalization. Whereas the function $\mathscr{L}_{\text{total}}$, in principle, provides the greatest sensitivity to M_A, the function $\mathscr{L}_{\text{FI}}$ is completely independent of the flux both in shape and normalization since the events themselves calibrate the energy and Q^2 distributions. The results of the fits are given in

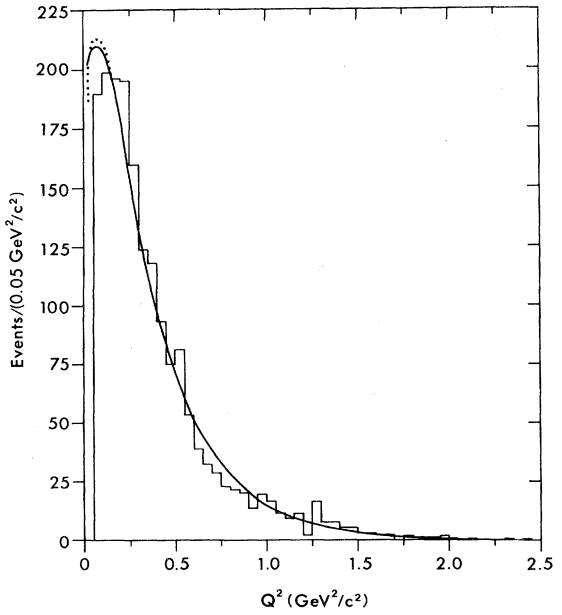

FIG. 4. Weighted Q^2 distribution. The solid curve is from a maximum-likelihood fit to the dipole model ($M_A = 1.00$ GeV/c^2). The dotted curve is from a fit to the AVMD model ($M_A = 1.11$ GeV/c^2).

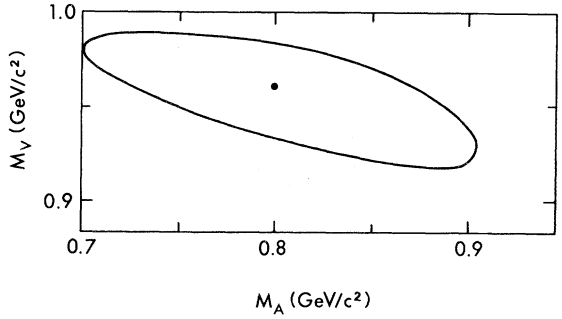

FIG. 5. Result of the two-parameter maximum-likelihood analysis using $\mathscr{L}_{\text{shape}}$ and dipole form factors. The curve is the one standard deviation contour.

TABLE I. Maximum-likelihood values of M_A (GeV/c^2) for each model.

	Monopole	Dipole	Tripole	QM-AVMD
Rate	0.45±0.11	0.74±0.12	0.95±0.16	0.69±0.26
Shape	0.57±0.05	1.05±0.05	1.38±0.06	1.25±0.17
Total	0.55±0.05	1.03±0.05	1.35±0.07	1.20±0.17
Flux independent	0.54±0.05	1.00±0.05	1.31±0.07	1.11±0.16

Table I. In all cases, results were found to be stable against various subdivisions of the data and our best value for M_A using the dipole parametrization and the function $\mathscr{L}_{\rm FI}$ is 1.00 ± 0.05 GeV/c^2 for $Q^2 \geq 0.05$ (GeV/c)^2.

Fits were also tried using monopole and tripole form factors. Both gave worse fits than obtained for the dipole form by at least 1.5 standard deviations.

As a test of CVC (conserved vector current) and the isotriplet-current hypothesis, we allowed the parameter M_V in the vector form factor to vary. In this test, we used $\mathscr{L}_{\rm shape}$ and dipole form factors. We found $M_A = 0.80\pm0.10$ GeV/c^2 and $M_V = 0.96\pm0.04$ GeV/c^2, as shown by the contour in the M_A:M_V space of Fig. 5. The errors quoted correspond to the diagonal elements of the error matrix and do not include the M_A:M_V correlations which is apparent in Fig. 5. This result for M_V is somewhat higher than the directly measured value of 0.84 GeV/c^2.

A functional form suggested by Sehgal[5] and motivated by the quark model and axial-vector-meson dominance (QM-AVMD), was tried:

$$F_A(Q^2) = \frac{-1.23}{(1+Q^2/M_A{}^2)} \exp\left[\frac{-Q^2R^2}{6(1+Q^2/4M_p{}^2)}\right],$$

where $R^2 = 6.00$ GeV^{-2} and M_p is the proton mass. This fit, shown as the dotted curve in Fig. 4, is better than the dipole by one standard deviation and gives an M_A value of 1.11 ± 0.16 GeV/c^2. The A_1 meson has a mass in the range 1.10 to 1.30 GeV/c^2 and a full width of 0.3 GeV/c^2. Thus, M_A for this model is consistent with the A_1 mass.

IV. CONCLUSIONS

Our result of $M_A = 1.00\pm0.05$ GeV/c^2 is in excellent agreement with the determination of 0.95 ± 0.09 GeV/c^2 obtained from the first experiment using the 12-foot bubble chamber.[2] It also agrees well with the recently published value of 1.07 ± 0.07 GeV/c^2 obtained using the 7-foot bubble chamber at the Brookhaven National Laboratory.[3]

We have recently analyzed the reaction $\nu_\mu p \to \mu^- p\pi^+$ and, within the context of the Adler model[4], obtained an independent measurement of M_A of $0.98^{+0.06}_{-0.03}$ GeV/c^2. Averaging the latter two results with the measurement of this paper gives $M_A = 1.01\pm0.03$ GeV/c^2 as the current best measurement from the neutrino experiments. Our data also agree well with the quark-model parametrization of Sehgal.

The axial-vector form factor can also be derived from threshold electropion production data by the application of PCAC and extrapolation to the pion pole. The different electroproduction experiments are not completely self-consistent and the results are also sensitive to the exact extrapolation method used. The recent analysis of Olsson *et al.*[6] concludes that the π^+ coincidence experiments are consistent with an M_A value of 1.15 ± 0.10 GeV/c^2, which is somewhat higher but not inconsistent with the neutrino results.

ACKNOWLEDGMENTS

We thank the operating crew of the 12-foot bubble chamber and the scanning and measuring staffs at the participating institutions for their cooperation during the last phases of a long bubble-chamber research program. The work was supported in part by the U. S. Department of Energy and the National Science Foundation.

*Present address: Gulf Science and Technology Company, Harmarville, PA 15024.
†Present address: U. S. Department of Energy, Washington, D.C. 20545.
‡Present address: Department of Physics, University of Toronto, Ontario, M5S 1A7, Canada.
§Present address: Louisiana State University, Baton Rouge, LA 70803.
||Permanent address: Valparaiso University, Valparaiso, IN 46383.
¶Present address: Bell Telephone Laboratories, Naperville, IL 60540.
**Present address: Rutgers University, New Brunswick, NJ 80903.
††Permanent address: Technion, Haifa, Israel.
‡‡Present address: Center for Naval Analyses, Alexandria, VA 22311.

[1]A review of the early experiments is given by M. Derrick, in *Proceedings of the Sixth International Symposium on Electron and Photon Interactions at High Energy, Bonn, Germany, 1973,* edited by H. Rollnik and W. Pfeil (North-Holland, Amsterdam, 1974), p. 369; S. Bonetti *et al.,* Nuovo Cimento 38A, 290 (1977); M. DeWit, in *Proceedings of the Topical Conference on Neutrino Physics at Accelerators, Oxford, 1978,* edited by A. G. Michette and P. B. Renton (Rutherford Laboratory, Chilton, Didcot, Oxfordshire, England 1978), p. 75.
[2]S. J. Barish *et al.,* Phys. Rev. D 16, 3103 (1977).
[3]N. J. Baker *et al.,* Phys. Rev. D 23, 2499 (1981).
[4]G. Radecky *et al.,* Phys. Rev. D 25, 1161 (1982).
[5]L. Sehgal, in *Proceedings of the European Physical Society International Conference on High Energy Physics, Geneva, 1979,* edited by A. Zichichi (CERN, Geneva, Switzerland), p. 98.
[6]M. G. Olsson, E. T. Osypowski, and E. H. Monday, Phys. Rev. D 17, 2938 (1978).